Hypoxia-sensing properties of the newborn rat ventral medullary surface *in vitro*

N. Voituron[1], A. Frugière[1,2], J. Champagnat[3] and L. Bodineau[1,2]

[1]*Laboratoire de Dysrégulations Métaboliques Acquises et Génétiques, UPRES EA 3901, Faculté de Médecine, Université de Picardie Jules Verne, 3 rue des Louvels, 80036 Amiens cedex 1, France*

[2]*Laboratoire de Neuropeptides Centraux et Régulations Hydrique et Cardiovasculaire, Inserm-U691, Collège de France, 11 place Marcelin Berthelot, 75231 Paris cedex 05, France*

[3]*Laboratoire de Neurobiologie Génétique et Intégrative, CNRS UPR 2216, Institut de Neurobiologie Alfred Fessard, Avenue de la Terrasse, 91198 Gif-sur-Yvette, France.*

The ventral medullary surface (VMS) is a region known to exert a respiratory stimulant effect during hypercapnia. Several studies have suggested its involvement in the central inhibition of respiratory rhythm caused by hypoxia. We studied brainstem–spinal cord preparations isolated from newborn rats transiently superfused with a very low O_2 medium, causing reversible respiratory depression, to characterize the participation of the VMS in hypoxic respiratory adaptation. In the presence of 0.8 mM Ca^{2+}, very low O_2 medium induced an increase in *c-fos* expression throughout the VMS. The reduction of synaptic transmission and blockade of the respiratory drive by 0.2 mM Ca^{2+} —1.6 mM Mg^{2+} abolished *c-fos* expression in the medial VMS (at the lateral edge of the pyramidal tract) but not in the perifacial retrotrapezoid nucleus/parafacial respiratory group (RTN/pFRG) VMS, suggesting the existence of perifacial RTN/pFRG hypoxia-sensing neurons. In the presence of Ca^{2+} (0.8 mM), lesioning experiments suggested a physiological difference in perifacial RTN/pFRG VMS between the lateral VMS (beneath the ventrolateral part of the facial nucleus) and the middle VMS (beneath the ventromedial part of the facial nucleus), at least in newborn rats. The lateral VMS lesion, corresponding principally to the most rostral part of the pFRG, produced hypoxia-induced stimulation, whereas the middle VMS lesion, corresponding to the main part of the RTN, abolished hypoxic excitation. This may involve relay via the medial VMS, which is thought to be the parapyramidal group.

(Resubmitted 16 April 2006; accepted after revision 8 August 2006; first published online 10 August 2006)
Corresponding author L. Bodineau: Laboratoire de Dysrégulations Métaboliques Acquises et Génétiques, UPRES EA 3901, Faculté de Médecine, Université de Picardie Jules Verne, 3 rue des Louvels, 80036 Amiens cedex 1, France.
Email: laurence.bodineau@u-picardie.fr

The ventral medullary surface (VMS) is known to be involved in chemical respiratory control, providing an adapted response to hypercapnia and hypoxia. During the 1960s, the pH-sensitive site (Mitchell *et al.* 1963) was thought to be responsible for the central hypercapnic stimulation of respiration (Mulkey *et al.* 2004; Guyenet *et al.* 2005*a*,*b*; Takakura *et al.* 2006). The VMS also seems to be involved in respiratory adaptation to hypoxia, consisting of an initial increase in respiration followed by a decrease (Vizek *et al.* 1987; Larnicol *et al.* 1994; Bodineau *et al.* 2000*a*,*b*). The initial increase is due primarily to an increase in the activity of peripheral O_2 chemoreceptors (Vizek *et al.* 1987). Hypoxic excitatory mechanisms have been detected in the pre-Bötzinger complex (Solomon *et al.* 2000). This hypoxic increase in respiratory drive increases the amount of O_2 taken in. The mechanisms responsible for the subsequent decrease probably originate in the brainstem and remain poorly understood (Vizek *et al.* 1987; Dillon *et al.* 1991; Voituron *et al.* 2005). It is thought that this decrease reflects the activation of 'central oxygen detectors' in the ventral medulla, actively inhibiting respiratory neurons (Reis *et al.* 1994; Sun & Reis, 1994; Neubauer & Sunderram, 2004; Pena *et al.* 2004). It has been shown that the VMS is specifically involved in the secondary decline in respiratory drive due to hypoxia (Bodineau *et al.* 2000*a*, 2001; Voituron *et al.* 2005). However, the reasons for respiratory stimulation during hypercapnia (Nattie, 1999; Mulkey *et al.* 2004; Guyenet *et al.* 2005*a*; Takakura *et al.* 2006) and for hypoxic respiratory depression by the VMS remain unclear. Some studies have provided evidence for the existence of pH- or CO_2-sensing neurons in the VMS

 DOI: 10.1113/jphysiol.2006.111765

(Okada *et al.* 2002; Mulkey *et al.* 2004; Guyenet *et al.* 2005*a*,*b*), but hypoxia-sensing properties remain to be demonstrated for VMS neurons. It has been suggested that hypoxia affects local metabolism and hypercapnic chemoreceptors (Nattie, 1999), although this seem unlikely as there is evidence to suggest that hypoxia and hypercapnia activate different structures (Belegu *et al.* 1999; Berquin *et al.* 2000; Okada *et al.* 2002; Voituron *et al.* 2005).

There is therefore a need to determine whether the neurons of the VMS have hypoxia-sensing properties and to characterize further the parts of the VMS involved in adaptation to hypoxia. The VMS contains several identified groups of neurons: the parafacial respiratory group (pFRG) and retrotrapezoid nucleus (RTN) in the perifacial VMS, and the parapyramidal group (PP) in a more medial position. The pFRG is a small cluster of pre-inspiratory neurons located in the lateral part of the VMS, in the most rostral area. It has recently been identified in neonates and is important for generating respiratory rhythm (Mellen *et al.* 2003; Onimaru & Homma, 2003; Borday *et al.* 2004; Onimaru *et al.* 2004, 2006; Janczewski & Feldman, 2006). It has been suggested that two distinct, independent respiratory oscillators are responsible for respiratory rhythm: the pFRG and the pre-Bötzinger complex (Mellen *et al.* 2003; Janczewski & Feldman, 2006; Onimaru *et al.* 2006). The pFRG is located close to the RTN, a thin layer of neurons located in the middle part of the VMS. The RTN has been defined in adult cats as a group of neurons projecting heavily into the ventral respiratory group and less heavily into the nucleus of the solitary tract (Smith *et al.* 1989). In adult rats, it was subsequently redefined as having a more caudal extension (Ellenberger & Feldman, 1990). As there is currently no known objective basis for anatomical or physiological distinction between RTN and pFRG, they are considered as a whole entity: the perifacial RTN/pFRG area (Onimaru & Homma, 2003; Weston *et al.* 2004; Guyenet *et al.* 2005*a*; Janczewski & Feldman, 2006; Takakura *et al.* 2006). The PP is located at the lateral edge of the pyramidal tract in the more medial part of the VMS (Connelly *et al.* 1989; Berquin *et al.* 2000; Pelaez *et al.* 2002; Stornetta *et al.* 2005). PP neurons have been reported to display tonic discharge (Mulkey *et al.* 2004) and to participate in autonomic regulatory processes such as thermogenic control (Blessing, 2005), defensive response to haemorrhage (Pelaez *et al.* 2002) and chemical respiratory reflexes (Erickson & Millhorn, 1994; Berquin *et al.* 2000; Okada *et al.* 2002).

The aim of this study on brainstem–spinal cord preparations was therefore to investigate the influence of the VMS on the central adaptation of respiratory rhythm to hypoxia. The pattern of expression of *c-fos*, the most effective marker of neuronal activation (Lanteri-Minet *et al.* 1994), revealed sensitivity to hypoxia following a decrease in synaptic transmission in the perifacial RTN–pFRG VMS, but not in the medial VMS containing the PP. Lesions of the lateral VMS led to hypoxia-induced stimulation, whereas lesions of the middle VMS abolished hypoxic excitation, possibly via a relay involving the medial VMS, thought to be the PP.

Methods

Experiments were carried out on 100 brainstem–spinal cord preparations from newborn (0–3 days old) Sprague Dawley rats (Janvier, Le Genest St Isle, France). All experiments were carried out in accordance with European Communities Council Directive of 24 November 1986 (86/609/EEC). All efforts were made to minimize the number of animals used and their suffering.

Surgery

Newborn rats were placed under deep ether anaesthesia and brainstem spinal–cord preparations were dissected out as described by Suzue (1984). Rostral cuts were made rostral to the fifth cranial nerve at the level of the superior cerebellar arteries and the caudal edge of the inferior colliculi. Caudal cuts were made between the seventh and eighth cervical spinal roots. Preparations were placed in a recording chamber (volume, 4 ml) with the ventral surface facing upward. They were continuously superfused, at a rate of 7.5 ml min^{-1}, at 26°C with oxygenated mock cerebrospinal fluid (oxygenated CSF (mM); 130.0 NaCl, 5.4 KCl, 0.8 $CaCl_2$, 1.0 $MgCl_2$, 26.0 $NaHCO_3$, 30.0 D-glucose) saturated with O_2 and adjusted to pH 7.4 by bubbling with 95% O_2 and 5% CO_2. The electrical activity of a C4 ventral root was recorded, using a suction electrode, filtered (10–3000 Hz), amplified ($\times$ 5000), integrated (time constant 100 ms) and digitized through a spike 2 data analysis system (CED, Cambridge, UK), at a sampling frequency of 1010 Hz. Respiratory frequency (Rf) was defined as the frequency of the bursts recorded from a C4 ventral root and the amplitude of the integrated C4 burst activity ($\int$C4) was used as an index of inspiratory activity (Suzue, 1984; Okada *et al.* 1998). These respiratory parameters stabilized between 5 and 10 min after surgery.

Experimental protocols

Very low O_2 conditions were created by replacing the oxygenated CSF with a solution of same composition bubbled with 95% N_2 and 5% CO_2 (anoxic CSF; pH 7.4). We used three experimental protocols: (i) an analysis of *c-fos* expression to determine the parts of the VMS activated by hypoxia, (ii) an analysis of central respiratory drive after destruction of the active areas identified in *c-fos* expression analysis, and (iii) a combination of the two first protocols: an analysis of the *c-fos* expression after selective destruction of the middle VMS. This protocol was

designed to test a hypothesis based on the data obtained with the two first protocols, as described in the results and discussion.

Protocol 1, analysis of *c-fos* expression. After 30 min of superfusion with oxygenated CSF, preparations were superfused with anoxic CSF for 30 min, as previously described (Bodineau *et al.* 2001; Voituron *et al.* 2005). Preparations were then fixed and processed for analysis of *c-fos* expression. Synaptic inputs were reduced, using a mock CSF with a low calcium and a high magnesium concentration (low Ca^{2+}–high Mg^{2+} CSF (mM); 130.0 NaCl, 5.4 KCl, 0.2 $CaCl_2$, 1.6 $MgCl_2$; 26.0 $NaHCO_3$, 30.0 D-glucose), in which the preparations were superfused in oxygenated (oxygenated-low Ca^{2+}–high Mg^{2+} CSF) and anoxic (anoxic-low Ca^{2+}–high Mg^{2+} CSF) conditions. The half-life of the Fos protein is between 90 and 100 min (Herdegen & Leah, 1998), and basal levels depend on the history of the preparation, including the surgical procedure used, in particular. Basal *c-fos* expression is maintained under reduced synaptic transmission, as previously described (Hausmann *et al.* 2001). We measured anoxia-induced *c-fos* expression by comparing preparations superfused with: oxygenated CSF for 60 min, $n = 8$; oxygenated CSF (30 min) → anoxic CSF (30 min), $n = 9$; oxygenated CSF (30 min) → oxygenated-low Ca^{2+}–high Mg^{2+} CSF (60 min), $n = 6$; oxygenated CSF (30 min) → oxygenated-low Ca^{2+}–high Mg^{2+} CSF (30 min) → anoxic-low Ca^{2+}–high Mg^{2+} CSF (30 min), $n = 8$.

We recorded C4 ventral root electrical activity and checked respiratory parameters to ensure that the preparations were alive. We carried out immunohistochemical analysis for the Fos protein immediately after these superfusions. Preparations were incubated in 4% paraformaldehyde in 0.1 M phosphate-buffered saline (pH 7.4) for 48 h at 4°C and then stored at −18°C in a cryoprotectant solution (5.4: 103 mM ethylene glycol, 86.0 mM NaCl, 172.0 mM polyvinyl pyrolidone, 876.0 mM saccharose in 0.1 M phosphate-buffered saline) for later use. Preparations were embedded in gelatin to facilitate the cutting of sections. Gelatin-embedded blocks were cooled and 40 μm sections were cut with a freezing microtome. Fos protein was detected using standard procedures for Fos-like immunohistochemistry. All histochemical procedures were performed on free-floating sections. Briefly, sections were placed in 0.1 M phosphate-buffered saline supplemented with 0.3% Triton X-100 and 2% normal goat serum. Sections were then incubated for 48 h at 4°C with a rabbit polyclonal antibody against the Fos protein (sc-52; Santa Cruz Biotechnology Inc., Santa Cruz, CA, USA) diluted 1/4000 in 0.1 M phosphate-buffered saline supplemented with 0.3% Triton X-100 and 1% normal goat serum. Sections were then incubated at room temperature for 2 h with a biotinylated goat anti-rabbit immunoglobulin diluted 1/200 and for 1 h with an avidin–biotin–peroxidase complex (Novostain Super ABC kit, Novocastra Laboratories, Newcastle, UK). Peroxidase activity was detected by incubating with 0.02% 3,3′-diaminobenzidine tetrahydrochloride, 0.04% nickel ammonium sulphate and 0.01% hydrogen peroxide in 0.05 M Tris buffer (pH 7.6). Sections were mounted in sequential caudo-rostral order on gelatin-coated slides, air-dried, dehydrated with absolute alcohol, cleared with xylene and coverslipped with Depex.

The specificity of the primary antibody was checked by the manufacturer (Santa Cruz Biotechnology Inc., Santa Cruz, CA, USA). No labelling was observed in the absence of the primary antibody against Fos protein.

The following tests were carried out to ensure that the effects of low Ca^{2+}–high Mg^{2+} CSF superfusion for 60 min were reversible: oxygenated CSF (30 min) → oxygenated-low Ca^{2+}–high Mg^{2+} CSF (60 min) → oxygenated CSF (30 min), $n = 3$; oxygenated CSF (30 min) → oxygenated-low Ca^{2+}–high Mg^{2+} CSF (30 min) → anoxic-low Ca^{2+}–high Mg^{2+} CSF (30 min) → oxygenated CSF (30 min), $n = 3$.

In both conditions, respiratory parameter values returned to control values during the recovery period (Fig. 1).

Protocol 2, respiratory parameter measurement. Respiratory parameters were measured on intact ($n = 19$) or lesioned ($n = 32$) preparations. Lesions were made in the VMS area displaying an increase in *c-fos* expression (protocol 1): the medial part of the VMS (at the lateral edge of the pyramidal tract; $n = 9$), the middle part of the VMS (ventromedial beneath the facial nucleus; $n = 11$) and the lateral part of the VMS (ventrolateral beneath the facial nucleus; $n = 12$). These areas were destroyed bilaterally, by the creation of an electrolytic lesion (direct current (DC) 200 μA, 1–2 s) with a tungsten microelectrode (Fig. 2). The following experiments were carried out: intact preparations: oxygenated CSF for 120 min, $n = 4$; oxygenated CSF (30 min) → anoxic CSF (30 min) → oxygenated CSF (30 min), $n = 15$. Lesioned preparations: oxygenated CSF (30 min) → lesion → oxygenated CSF (30 min) → anoxic CSF (30 min) → oxygenated CSF (30 min).

As for protocol 1, we recorded the electrical activity of the C4 ventral root with a suction electrode. We observed no change in the respiratory parameters, Rf and $\int$C4, in intact preparations superfused with oxygenated CSF for 120 min. We checked the extent of the lesions as follows. Preparations were incubated in a fixative solution of 4% paraformaldehyde in 0.1 M phosphate buffer (pH 7.4) for 48 h at 4°C and then embedded in gelatine. Gelatine blocks were cut into 40 μm sections with a freezing microtome. Sections were stained with cresyl violet,

examined under a microscope to locate the lesion and photographed, using a digital camera fixed to the microscope (magnification × 100; Fig. 2). The extent of lesion was expressed as a percentage of the whole cluster of neurons expressing *c-fos* when preparations were superfused with anoxic CSF.

Protocol 3, analysis of *c-fos* expression after selective destruction of the middle part of the VMS. This protocol was designed to assess interactions between the middle VMS and the medial VMS in anoxic conditions. We assessed the consistency of this interaction, by evaluating *c-fos* expression after the generation of lesions in the middle VMS ($n = 12$). Bilateral areas were destroyed, as in protocol 2, by an electrolytic lesion (DC 200 μA, 1–2 s) with a tungsten microelectrode. The following experiments were carried out: oxygenated CSF (30 min) → lesion → oxygenated CSF (60 min), $n = 6$; oxygenated CSF (30 min) → lesion → oxygenated CSF (30 min) → anoxic CSF (30 min), $n = 6$.

C4 ventral root electrical activity was recorded and respiratory parameters were checked to ensure that preparations were alive. Middle VMS lesions induced similar changes in mean Rf ($P < 0.1$) and mean $\int$C4 ($P < 0.3$) as were induced in protocol 2. Preparations were then immediately incubated in 4% paraformaldehyde in 0.1 M phosphate-buffered saline (pH 7.4) and immunohistochemical analysis for Fos protein was conducted on free-floating sections, as in protocol 1. After immunohistochemical treatment, sections were stained with neutral red and, as in protocol 2, the extent of lesions was checked and expressed as a percentage of the whole cluster of neurons expressing *c-fos* when preparations were superfused with anoxic CSF.

Data and statistical analysis

All values are expressed as mean ± standard error of the mean (S.E.M.).

Anatomical study. Sections were examined under a light microscope in sequential caudo-rostral order. Sections from all the brainstems were aligned, to ensure that cell counts concerned the same part of VMS. This alignment was based on a reference section: the section containing the most rostral part of the facial nucleus. Cells were counted in sections caudal to this reference

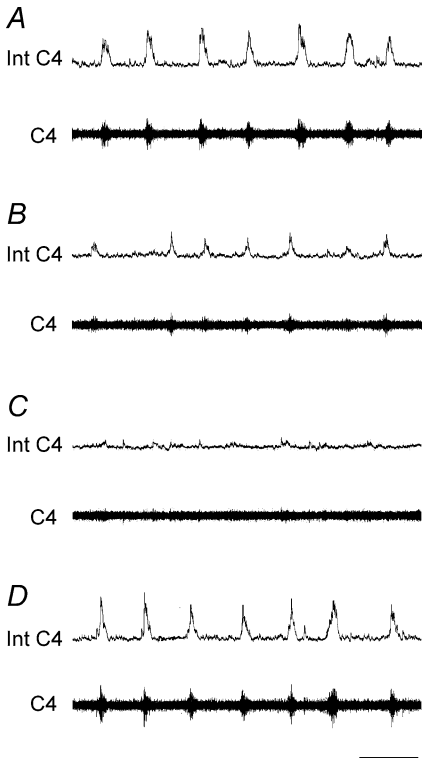

Figure 1. Changes in central respiratory drive induced by reduced synaptic transmission
Superfusion with low Ca^{2+}–high Mg^{2+} CSF progressively abolishes central respiratory drive. Respiratory C4 activity under superfusion with oxygenated CSF (*A*), 10 min (*B*) and 25 min (*C*) after the start of superfusion with low Ca^{2+}–high Mg^{2+} CSF and 15 min after the return to oxygenated CSF superfusion (*D*). Int C4, integrated C4 activity (upper traces); C4, C4 activity (lower traces); scale bar, 10 s.

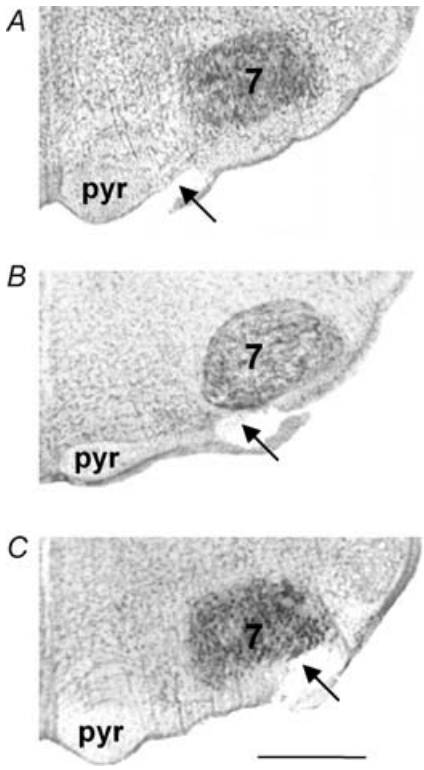

Figure 2. Location of the ventral medullary surface lesions
Photomicrographs of the ventral medulla, showing a lesion of the medial VMS (*A*), middle VMS (*B*) and lateral VMS (*C*). Abbreviations: 7, facial nucleus; pyr, pyramidal tract. Scale bar, 500 μm.

section. The distribution of Fos-like immunoreactive (FLI) neurons at the ventral medullary surface was plotted with the aid of a drawing tube attached to the microscope (magnification × 40). Fos-positive neurons were also photographed, using a digital camera fixed to the microscope (magnification × 100), and counted by eye at high magnification (× 200), in blind conditions. VMS cell counts were obtained in several steps. Firstly, cells were counted throughout the medulla, in preparations superfused with oxygenated CSF and anoxic CSF. Secondly, when experimental conditions were known, we preferentially distinguished the rostro-caudal extents of Fos-positive neurons in the three subdivisions of the VMS in anoxic conditions: (i) lateral VMS, 400 μm from the rostral part of the facial nucleus (10 sections), (ii) middle VMS, on 600 μm from the rostral part of the facial nucleus (15 sections), and (iii) medial VMS, on 600 μm from the rostral part of the facial nucleus (15 sections). We then compared the number of neurons in the same rostro-caudal areas in oxygenated and anoxic conditions. For all other groups of preparations, low Ca^{2+}–high Mg^{2+} superfusions (oxygenated and anoxic) and preparations with middle VMS lesions (oxygenated and anoxic), we analysed Fos labelling strictly at the rostro-caudal levels defined at the outset. We counted Fos-positive neurons on one entire side of the neuraxis for the facial nucleus and over the entire area for the raphe pallidus nucleus (RPa). We analysed differences between the mean numbers of neurons per section and per area (parts of the VMS, RPa and facial nucleus) obtained in previously described situations, using one-way analysis of variance (ANOVA) followed by Fisher's *post-hoc* least squares differences (PLSD) correction. Data were considered significant if $P < 0.05$.

Respiratory parameter analysis. We determined control values during the 10 min preceding the test. Rf and $\int$C4 were averaged over successive 5 min periods and expressed as a percentage of control values. We used this procedure to evaluate (i) the mean effect of the lesions and (ii) the mean effect of anoxic superfusion on respiratory parameters. Only one exposure to anoxia was studied for each preparation. The anoxic test was repeated with several preparations to determine the mean effect on Rf and $\int$C4, and several comparisons were made. First, we compared mean Rf and mean $\int$C4 control values with those obtained after lesioning. Second, we compared the values obtained in anoxic conditions with control and pre-anoxic values (the 10 min preceding the anoxic test) for the three preparations with VMS lesions (medial, middle and lateral parts of the VMS). Third, we compared changes under anoxic conditions in mean Rf and mean $\int$C4 between the various types of preparation (each preparation compared systematically with the others: intact and lesioned preparations). We determined the significance of any differences by Student's paired *t* test for the two first comparisons and by ANOVA followed by Fisher's PLSD correction for the third comparison. Differences were considered significant if $P < 0.05$.

Results

c-fos expression in oxygenated and anoxic conditions

Under oxygenated conditions ($n = 8$), we observed basal levels of *c-fos* expression in all parts of the VMS (medial, middle and lateral), and in the adjacent RPa and facial nucleus (Figs 3 and 4; Table 1). After superfusion of the preparations with anoxic CSF ($n = 9$), *c-fos* expression

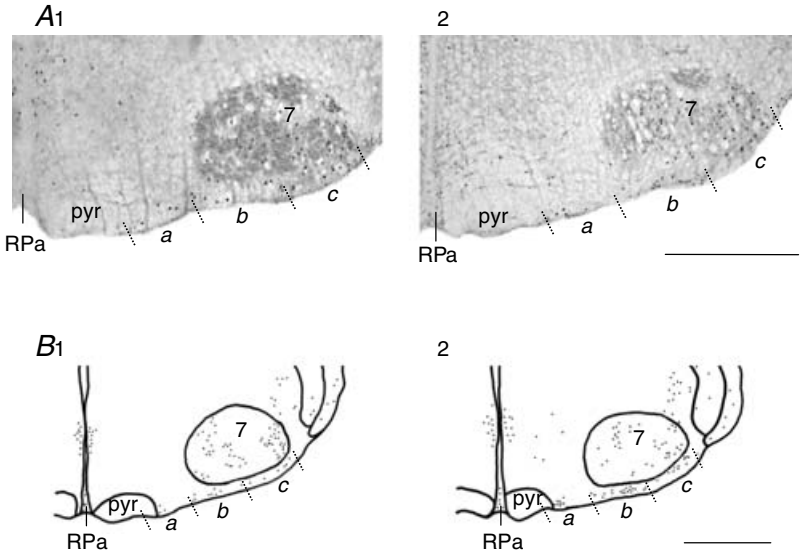

Figure 3. Representative labelling illustrating changes in *c-fos* expression induced by anoxia in conditions of active and reduced synaptic transmission
C-*fos* expression in medial VMS (*a*), middle VMS (*b*), lateral VMS (*c*) and adjacent areas, under oxygenated and anoxic conditions. Photomicrographs showing FLI neurons in oxygenated-low Ca^{2+}–high Mg^{2+} CSF (*A*1) and anoxic-low Ca^{2+}–high Mg^{2+} CSF (*A*2). FLI neuron distribution in preparations superfused with oxygenated CSF (*B*1) and anoxic CSF (*B*2). Abbreviations: 7, facial nucleus; RPa, raphe pallidus nucleus; pyr, pyramidal tract. Scale bar, 500 μm.

Table 1. *C-fos* expression in VMS and adjacent areas

	Classic CSF		Low Ca^{2+}–high Mg^{2+} CSF		Middle VMS lesion	
	Oxygenated $n = 8$	Anoxic $n = 9$	Oxygenated $n = 6$	Anoxic $n = 8$	Oxygenated $n = 6$	Anoxic $n = 6$
		a	b	a, c	d, e	a, f, g
Raphe pallidus nucleus	7.4 ± 2.0	5.5 ± 0.8 n.s.	6.8 ± 0.4 n.s.	6.9 ± 0.5 n.s., n.s.	8.2 ± 1.3 n.s., n.s.	8.8 ± 0.6 n.s., n.s., n.s.
Medial VMS	3.1 ± 0.3	6.8 ± 0.3 $P < 0.0001$	2.7 ± 0.2 n.s.	2.9 ± 0.3 n.s., $P < 0.0001$	2.6 ± 0.5 n.s., n.s.	2.5 ± 0.2 n.s., $P < 0.0001$, n.s.
Perifacial RTN/pFRG VMS	15.3 ± 0.6	29.1 ± 2.0 $P < 0.03$	15.8 ± 0.3 n.s.	26.3 ± 2.6 $P < 0.004$, n.s.	—	—
Middle VMS	8.5 ± 0.8	19.4 ± 2.8 $P < 0.005$	9.8 ± 0.4 n.s.	15.8 ± 2.8 $P < 0.05$, n.s.	—	—
Lateral VMS	6.8 ± 0.4	9.7 ± 1.1 $P < 0.05$	6.0 ± 0.3 n.s.	10.5 ± 0.7 $P < 0.0003$, n.s.	5.9 ± 0.9 n.s., n.s.	11.2 ± 0.6 $P < 0.0001$, n.s., n.s.
Facial nucleus	71.6 ± 3.5	69.5 ± 5.1 n.s.	68.1 ± 8.2 n.s.	68.3 ± 3.7 n.s., n.s.	62.0 ± 5.7 n.s., n.s.	62.2 ± 0.6 n.s., n.s., n.s.

Values are mean number (± S.E.M.) of FLI neurons/section. *a*, indicates comparison between oxygenated and anoxic conditions for classic, low Ca^{2+}–high Mg^{2+} CSF and middle VMS lesion; *b*, indicates comparison between classic and low Ca^{2+}–high Mg^{2+} CSF oxygenated conditions; *c*, indicates comparison between classic and low Ca^{2+}–high Mg^{2+} CSF anoxic conditions; *d*, indicates comparison between classic-CSF and middle VMS lesion in oxygenated conditions; *e*, indicates comparison between low Ca^{2+}–high Mg^{2+} CSF and middle VMS lesion in oxygenated conditions; *f*, indicates comparison between classic CSF and middle VMS lesion in anoxic conditions; *g*, indicates comparison between low Ca^{2+}–high Mg^{2+} CSF and middle VMS lesion in anoxic conditions. n.s., not significant.

was found to have increased in all the parts of the VMS. The number of Fos-positive neurons was 50% higher in the lateral VMS on 400 μm of rostro-caudal extension ($P < 0.05$) and about 130% higher in the middle VMS on 600 μm of rostro-caudal extension ($P < 0.005$) in anoxic than in oxygenated conditions. This resulted in 90% higher levels of perifacial RTN/pFRG *c-fos* expression ($P < 0.03$) in anoxic conditions. Besides,

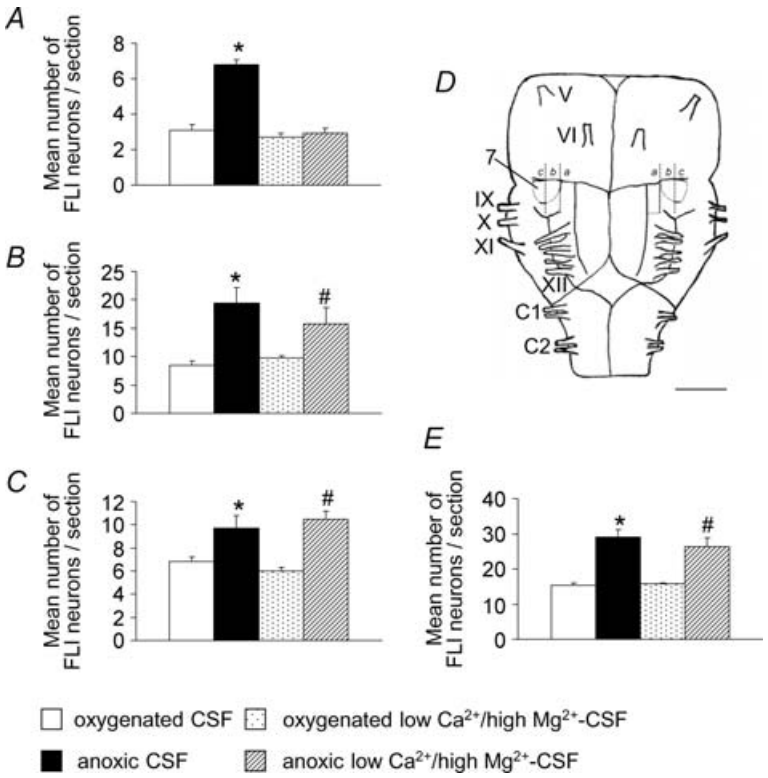

Figure 4. Histograms showing the mean changes in *c-fos* expression induced by anoxia in conditions of active and reduced synaptic transmission
Mean number of FLI neurons per section in the medial (*A*), middle (*B*), lateral (*C*) and perifacial RTN/pFRG (*E*) VMS in oxygenated and anoxic conditions, under conditions of active and reduced synaptic transmission. Significant changes induced by anoxic conditions are indicated by * under intact synaptic transmission conditions and # under reduced synaptic transmission conditions ($P < 0.05$). Schematic diagram of a ventral view of the brainstem and the two first segments of the spinal cord (*D*) indicating the distribution of anoxic Fos-positive neurons in the three parts of the VMS (*a*, medial; *b*, middle and *c*, lateral in Fig. 2) in conditions of active synaptic transmission (left) and reduced synaptic transmission (right). 7, facial nucleus; V–XII, cranial nerves; C1, C2, cervical ventral roots. Scale bar, 1 mm.

c-fos expression was 120% higher in the medial VMS on 600 μm of rostro-caudal extension ($P < 0.0001$; Figs 3*B* and 4, Table 1) in anoxic than in oxygenated conditions. By contrast, *c-fos* expression remained unchanged in the adjacent RPa and facial nucleus (Fig. 3*B*, Table 1).

We reduced synaptic transmission by superfusing preparations with a low Ca^{2+}–high Mg^{2+} CSF, to investigate whether the increase in *c-fos* expression in the VMS was due to intrinsic neuronal properties or to synaptic connections with O_2-sensitive areas. In oxygenated conditions, C4 activity decreased 6–10 min after synaptic transmission was reduced and was totally abolished 11–15 min later ($n = 9$; Fig. 1). No change in *c-fos* expression was observed in the VMS and adjacent areas, the RPa and facial nucleus ($n = 6$; Figs 3*A* and 4, Table 1). In conditions of reduced synaptic transmission, the increase in *c-fos* expression induced by anoxia was observed in the perifacial RTN/pFRG VMS ($P < 0.004$): in the middle ($P < 0.05$) and lateral ($P < 0.0003$; Figs 3*A* and 4*B*–*E*, Tables 1, $n = 8$) parts. By contrast, no increase in *c-fos* expression was observed in the medial VMS (Figs 3*A*, and 4*A* and *E*, Tables 1, $n = 8$). We conclude that cells in the perifacial RTN/pFRG VMS are directly sensitive to a decrease in the O_2 content of mock CSF.

Different respiratory control modes originating in the VMS

Under control conditions, the mean Rf was 6.8 ± 0.3 bursts min^{-1}.

Effect of ventral medullary area lesions on baseline respiratory parameters. We specifically lesioned the VMS at three different lateral points of the medial axis: the medial, middle and lateral parts of the VMS, as described in the experimental protocols (Fig. 2). We then analysed changes in respiratory parameters, to assess the effects on respiration on these parts of the VMS, which show an increase in *c-fos* expression in response to anoxia. Mean lesion size was 240 ± 23 μm, corresponding to the destruction of ∼60% of the lateral VMS showing an increase in *c-fos* expression and ∼40% of the middle and medial VMS showing an increase in *c-fos* expression. Lateral VMS lesions induced a decrease in the two respiratory parameters evaluated – mean Rf and mean $\int$C4 – whereas lesions of the middle VMS induced only a decrease in mean $\int$C4 and lesions of the medial VMS induced only an increase in mean Rf.

We therefore observed a decrease in mean Rf and mean $\int$C4 after lesioning of the lateral VMS ($n = 12$). Mean Rf and mean $\int$C4 decreased to $84.4 \pm 4.8\%$ ($P < 0.009$) and $89.8 \pm 3.4\%$ ($P < 0.04$) of control values, respectively, within 5 min of lesioning. No subsequent changes were observed (mean Rf and mean $\int$C4 were at $79.7 \pm 2.8\%$ ($P < 0.0002$) and $87.2 \pm 4.2\%$ ($P < 0.02$) of control values, respectively, after 20 min). Lesioning of the middle VMS was followed by a decrease in mean $\int$C4, with no significant change in Rf. Thus, mean $\int$C4 was $89.5 \pm 2.0\%$ of control values ($P < 0.05$) 5 min after lesioning of the middle VMS ($n = 23$). We observed no significant change after this time (mean $\int$C4 was $83.4 \pm 2.4\%$ of control values after 20 min; $P < 0.02$).

Conversely, we observed an increase in mean Rf after destroying the medial VMS, reaching $118.9 \pm 5.5\%$ of control values 25 min after lesioning ($P < 0.02$; $n = 9$).

Effect of ventral medullary area lesions on hypoxic central respiratory adaptation. In intact preparations, decreasing the O_2 content of the mock CSF led to a decrease in mean Rf, with no change in mean $\int$C4 ($n = 15$; Figs 5*A* and 6*A*). Mean Rf started to decrease 6–10 min after the initiation of superfusion with anoxic CSF ($87.4 \pm 4.6\%$ of control values; $P < 0.006$) and reached $73.6 \pm 3.1\%$ of control values ($P < 0.0001$) between 16 and 30 min after the onset of anoxic conditions. Mean Rf returned to control values during the recovery period.

The exposure to anoxia of preparations lesioned in the middle VMS ($n = 11$) and in the medial VMS ($n = 9$) rapidly resulted in an acceleration of respiratory rhythm not observed in intact preparations (Figs 5*B* and *C*, 6*B* and *C*, and 7). After the first 5 min of anoxia, mean Rf was $128.5 \pm 11.3\%$ ($P < 0.02$) and $147.6 \pm 16.7\%$ ($P < 0.02$) of control values for preparations lesioned in the middle VMS and in the medial VMS, respectively. Increases in mean Rf were not significantly different ($P < 0.2$) for these preparations. Mean Rf remained higher over the next 10 min ($108.8 \pm 11.4\%$ of control values; $P < 0.01$) in preparations with medial VMS lesions than in intact preparations. During the rest of the period of exposure to anoxia, mean Rf values were similar to those for intact preparations, at 78.2 ± 4.2 and $87.7 \pm 10.6\%$ of control values between 16 and 30 min of anoxia for preparations with middle VMS and medial VMS lesions, respectively. As for intact preparations, we observed no significant change in mean $\int$C4 for either of the two lesioned preparations (Fig. 5*B* and *C*). Mean Rf returned to control values during the recovery period.

Preparations with lateral VMS lesions ($n = 12$) had a different pattern of respiratory adaptation to anoxic conditions than in intact preparations or preparations with medial or middle VMS lesions (Figs 5*D*, 6*D* and 7), with mean Rf remaining significantly lower than pre-anoxic values throughout the entire period of exposure to anoxia ($P < 0.05$). Mean Rf decreased to $71.9 \pm 4.0\%$ of control values ($P < 0.0001$) within the first 5 min of anoxia, remaining unchanged in intact preparations and increasing in preparations with lesions in the medial or middle VMS. Over the next 5 min, mean Rf decreased to a greater extent in these lesioned preparations ($68.6 \pm 5.2\%$ of control values, $P < 0.0001$) than in intact preparations.

For the rest of the period of exposure to anoxia, the decrease in mean Rf was similar to those for intact preparations and preparations with medial and middle VMS lesions ($72.9 \pm 3.5\%$ of control values after 16–30 min of anoxic conditions). Anoxic conditions did not affect the mean $\int$C4, which remained at the level observed after lesioning ($81.4 \pm 6.1\%$ of control values; $P < 0.008$; Fig. 5*D*). Mean Rf returned to pre-anoxic values during the recovery period.

Effect of the middle VMS lesion on *c-fos* expression in the other parts of the VMS. Specific destruction of middle VMS modified the pattern of *c-fos* expression induced by anoxia in the medial VMS (Table 1).

On preparations with middle VMS lesions superfused with oxygenated CSF ($n = 6$), we observed no change in *c-fos* expression in the medial or lateral VMS or in the RPa and facial nucleus. Superfusion of the preparations with anoxic CSF ($n = 6$) increased *c-fos* expression only in the lateral VMS ($P < 0.0001$). Thus, destruction of the middle VMS abolished the increase in *c-fos* expression observed in the medial VMS in the presence of an intact middle VMS.

Discussion

In this study, we identified hypoxia-sensing neurons in the perifacial RTN/pFRG VMS. The RTN, located in the middle VMS, beneath the ventromedial part of the facial nucleus (Ellenberger & Feldman, 1990), is known to act as a chemoreceptor in CO_2 detection (Nattie, 1999; Mulkey *et al.* 2004; Guyenet *et al.* 2005*a*; Takakura *et al.* 2006) and to express *c-fos* in rats exposed to hypercapnia (Teppema *et al.* 1997; Okada *et al.* 2002). The pFRG, located in the lateral VMS in its most rostral part, beneath the ventrolateral part of the facial nucleus, is a cluster of pre-inspiratory neurons recently described in neonates and shown to be important in the generation of respiratory rhythm, at least in neonates (Mellen *et al.* 2003; Onimaru & Homma, 2003; Borday *et al.* 2004; Janczewski & Feldman, 2006). Lesioning of the lateral VMS, corresponding mostly to the most rostral part of the pFRG (Onimaru & Homma, 2003), suggests that this area generated anoxia-induced stimulation. By contrast, lesioning of the middle VMS, housing the RTN (Ellenberger & Feldman, 1990), abolished anoxic excitation, possibly via a relay involving the medial VMS, which is thought to be the PP (Connelly *et al.* 1989; Pelaez *et al.* 2002; Stornetta *et al.* 2005).

General observations

Brainstem–spinal cord preparation. Experiments were performed on brainstem–spinal cord preparations isolated

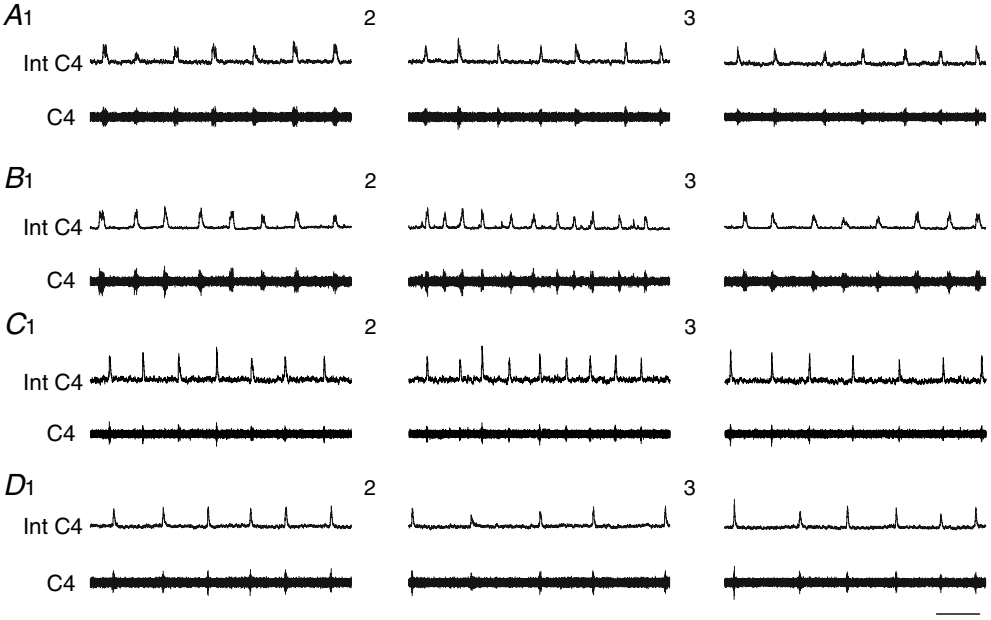

Figure 5. Anoxic central respiratory drive adaptation in intact preparations and preparations with VMS lesions
Differences in anoxic respiratory drive adaptation in intact preparations (*A*), and preparations with medial (*B*), middle (*C*) and lateral (*D*) VMS lesions. The column on the left corresponds to the pre-anoxic period (*A*1, *B*1, *C*1, *D*1), the middle column corresponds to the first 10 min of anoxia (*A*2, *B*2, *C*2, *D*2) and the column on the right corresponds to the recovery period (*A*3, *B*3, *C*3, *D*3). Int C4, integrated C4 activity (upper traces); C4, C4 activity (lower traces); scale bar, 10 s.

en bloc from newborn rats; such preparations generate a rhythmic activity closely resembling central respiratory drive (Suzue, 1984). A P_{O_2} gradient has been shown to exist, but respiratory neurons have been assumed to function under aerobic conditions (Brockhaus *et al.* 1993; Okada *et al.* 1993). One advantage of the approach used here is that this totally deafferented brainstem–spinal cord preparation constitutes an appropriate model for investigating central mechanisms involved in respiratory adaptation to hypoxia. In previous studies (Okada *et al.* 1998; Bodineau *et al.* 2000*a*, 2001; Voituron *et al.* 2005), as in this report, brainstem–spinal cord preparations have been shown to display a decrease in Rf in very low O_2 conditions that is reversed by reoxygenation. Thus, neurons subjected to anoxic conditions during the test seem to be viable when transferred to control conditions.

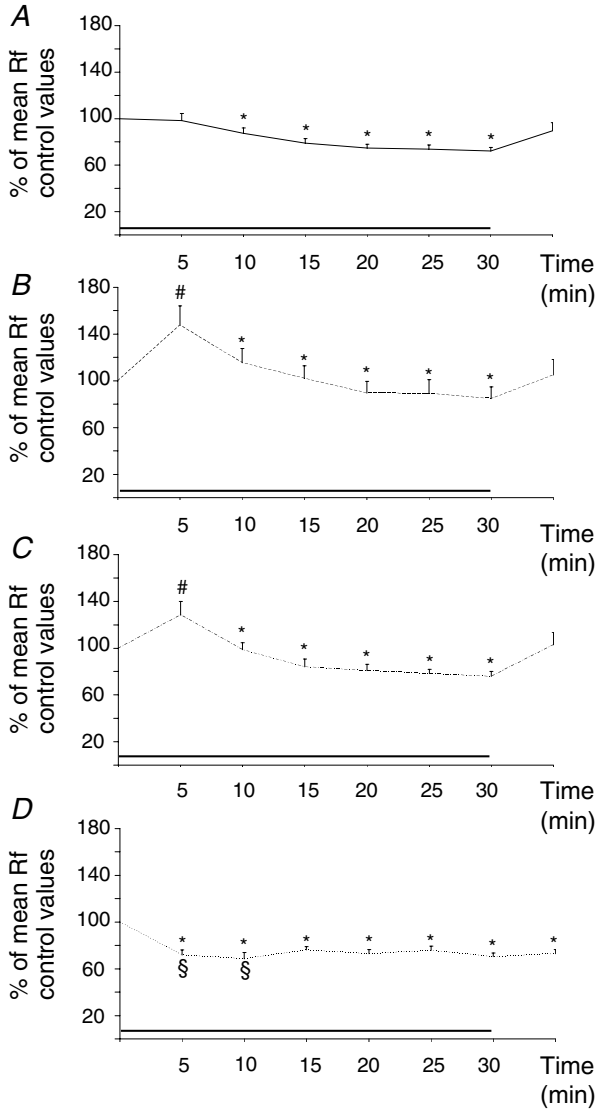

Figure 6. Changes in mean Rf induced by anoxia in intact preparations and preparations with VMS lesions
Two different anoxic respiratory control modes exerted by the VMS. Effect of exposure to anoxia (black bar) on mean Rf in intact preparations (*A*), and preparations with lesions in the medial (*B*), middle (*C*), and lateral (*D*) VMS. Each point corresponds to the average for a 5 min recording period. * indicates a decrease in mean Rf with respect to control values for all types of preparation ($P < 0.05$), # indicates an increase in mean Rf with respect to intact preparations for medial- and middle-lesioned preparations ($P < 0.05$), and § indicates a decrease in mean Rf with respect to intact preparations for lateral VMS-lesioned preparations ($P < 0.05$).

C-fos expression analysis. *C-fos* is an immediate early gene, and the detection of its product, Fos protein, is classically used to identify neuronal populations involved in specific respiratory responses *in vivo* (Teppema *et al.* 1997; Berquin *et al.* 2000; Bodineau & Larnicol, 2001; Takakura *et al.* 2006) and *in vitro* (Bodineau *et al.* 2001; Okada *et al.* 2002; Saadani-Makki *et al.* 2004; Voituron *et al.* 2005). Although some neurons do not seem to express the *c-fos* gene (Dragunow & Faull, 1989), this method has proved useful for the determination of neural pathways, such as those involved in respiratory rhythm adaptation. As Fos protein may have a half-life of 90–100 min (Herdegen & Leah, 1998), basal levels may be strongly affected by the history of the preparation, including surgical procedures, for example. We used a 30 min anoxia period, corresponding to that used for the analysis of respiratory adaptation to low O_2 conditions in brainstem–spinal cord preparations (Okada *et al.* 1998; Bodineau *et al.* 2000*a*, 2001; Voituron *et al.* 2005). This period is long enough for the induction of detectable changes in *c-fos* expression in response to neuronal activation during the first minute of exposure to anoxia (Morgan *et al.* 1987; Sagar *et al.* 1988; Herdegen *et al.* 1991). Indeed, it has been shown that 5 min of stimulation are sufficient to induce changes in *c-fos* expression, which are observed after a latent period of 15–20 min (Marina *et al.* 2002). Thus, the *c-fos* expression changes observed in our study probably reflect changes

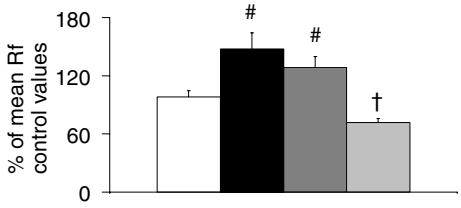

Figure 7. Effect of VMS lesions on Rf at the start of exposure to anoxia
Histogram showing the mean Rf of intact preparations (white bar), and preparations with medial (black bar), middle (dark grey bar) and lateral (light grey bar) VMS lesions for the first 5 min of exposure to anoxia. # indicates an increase in mean Rf with respect to intact preparations for medial VMS- and middle VMS-lesioned preparations ($P < 0.05$), and † indicates a decrease in mean Rf with respect to intact preparations for lateral VMS-lesioned preparations ($P < 0.05$).

in neuronal activity occurring within the first 10 min of respiratory adaptation to very low O_2 conditions. If neurons anywhere in the brainstem–spinal cord present changes in activity later in the period of exposure to anoxia, these changes cannot be detected by *c-fos* analysis.

Lesioning experiments. Selective discrete lesions were created throughout the VMS: in its medial, middle and lateral parts. The areas destroyed were smaller than the areas displaying changes in *c-fos* expression in response to anoxia. The contribution of the VMS was thus minimized. However, the destruction of ∼60% of the lateral VMS and ∼40% of the middle and medial VMS are sufficient to alter certain respiratory parameters. The areas selectively destroyed were neighbouring areas, raising the question of the effects of neural damage in parts of the VMS located in the vicinity of the lesion. Following lesioning of the middle VMS, we observed no change in basal *c-fos* expression in the neighbouring lateral or medial VMS, suggesting that lesions do not affect adjacent parts of the VMS. In addition, as electrolytic lesions destroy both pools of neurons in the targeted region and axons of neural pathways passing through the area, the interpretation of results may be difficult. When the lateral VMS is lesioned, some neuronal fibres originating from the A5 region may also be destroyed. As previously demonstrated (Hilaire *et al.* 1989, 2004), destruction of the A5 region induces an increase in Rf by abolishing the moderator control exerted by the noradrenergic A5 neurons. We demonstrate here a decrease in Rf after lesioning of the lateral VMS. It therefore seems unlikely that the observed effect depends on the destruction of these A5 neuronal fibres. The medial VMS has been shown to be crossed by neurons descending from the hypothalamic and midbrain structures (Beitz, 1995; Simerly, 1995). In the brainstem–spinal cord preparation studied here, which lacked supra-pontine areas, this interruption of neural pathways is unlikely to be responsible for the observed effects. It would also appear unlikely that the possible destruction of connections between the dorsal pons and the ventral column, passing through the VMS, are responsible for the difference in respiratory drive adaptation to very low O_2 conditions because, as previously reported, no pontine regions seem to be activated by anoxia in these *in vitro* conditions (Voituron *et al.* 2005).

Hypoxia-sensing properties of the VMS

Very low O_2 conditions induced an increase in *c-fos* expression in the VMS that was not affected by a decrease in synaptic transmission in the perifacial RTN/pFRG VMS and was abolished in the adjacent medial VMS. This suggests that hypoxia is directly detected by cells in the perifacial RTN/pFRG VMS.

The molecular basis of direct central hypoxia detection is unknown. Mulkey *et al.* (2004) recently identified a pH-sensitive K^+ current contributing to the CO_2 chemosensitivity of RTN neurons suggested by the results of previous studies (Teppema *et al.* 1997; Li & Nattie, 2002; Okada *et al.* 2002). Mulkey *et al.* (2004) and Guyenet *et al.* (2005*a*,*b*) suggested that this current may involve TASK channels. TASK channels have been implicated in peripheral chemoreceptor functioning in both O_2- and pH-sensing mechanisms (Patel & Honore, 2001). They may therefore be involved in the detection of hypoxia by perifacial RTN/pFRG neurons, but this hypothesis remains to be tested. Alternatively, the population of hypoxia-sensing neurons may be different from the population of CO_2-sensing neurons. For example, HERG-like K^+, K_{ATP} or Ca^{2+}-activated K^+ channels are thought to be involved in O_2 sensitivity (Overholt *et al.* 2000; López-Barneo *et al.* 2004; Mironov *et al.* 2005) and may play a part in the hypoxia-sensing properties of perifacial RTN/pFRG VMS. Alternatively, ATP, which is released in the VMS, may be involved, leading to the hypoxia-induced slowing of Rf (Gourine *et al.* 2005). The possible involvement of such a mechanism in the hypoxia-sensing properties of perifacial RTN/pFRG VMS should also be considered.

Our results and those of previous studies (Teppema *et al.* 1997; Li & Nattie, 2002; Okada *et al.* 2002; Mulkey *et al.* 2004; Guyenet *et al.* 2005*a*,*b*; Kawai *et al.* 2006; Takakura *et al.* 2006) suggest that perifacial RTN/pFRG VMS is a major site for the chemical control of respiration. As it innervates the region of the pre-Bötzinger complex and the rostral part of the ventral respiratory group (Pearce *et al.* 1989; Smith *et al.* 1989; Weston *et al.* 2004), the perifacial RTN/pFRG VMS may be a source of integrated chemical drive playing a major role in respiratory adaptation to hypoxic and hypercapnic conditions.

The lateral VMS, but not the adjacent middle and medial VMS, stimulates respiration in very low O_2 conditions

In oxygenated baseline conditions, bilateral lesions of the lateral VMS decreased both Rf and $\int$C4. These findings are consistent with those of Onimaru & Homma (2003). This positive influence on Rf is consistent with the glutamatergic character of perifacial RTN/pFRG VMS neurons (see Figs 2*H* and 4 in Weston *et al.* 2004). Similarly, bilateral destruction of the middle VMS, which also contains glutamatergic neurons (Weston *et al.* 2004), decreased $\int$C4. This depressive effect of middle VMS lesions suggests that the positive respiratory influence of this region linked to its reported CO_2-sensing properties (Nattie, 1999; Mulkey *et al.* 2004; Guyenet *et al.* 2005*a*) affected only $\int$C4 in our experimental conditions. By

contrast, bilateral lesion of the medial VMS increased Rf, suggesting that medial VMS neurons inhibit respiratory rhythm generation. This is consistent with the GABAergic nature of these neurons (Weston *et al.* 2004; Stornetta *et al.* 2005).

In anoxic conditions, lesions of the middle or medial VMS revealed an early acceleration of Rf not observed in intact preparations, whereas lesions of the lateral VMS accentuated the decrease in Rf in anoxic conditions. We suggest that the early anoxic stimulation caused by lesions of the middle or medial VMS is linked to the activation of intact lateral VMS neurons. Lateral VMS neurons increase Rf during anoxia through direct sensitivity to hypoxia.

The medial VMS causes anoxic depression and eliminates anoxic excitation

As previously reported, the *in vitro* hypoxic decrease in Rf was accompanied by an increase in *c-fos* expression in the middle and medial VMS in the presence of active synaptic transmission (Bodineau *et al.* 2001; Voituron *et al.* 2005). This is consistent with *in vivo* studies performed in adult cats and rats showing that this part of the VMS is involved in central respiratory hypoxic adaptation (Bodineau *et al.* 2000*b*; Bodineau & Larnicol, 2001). RTN neurons in the middle VMS increase their firing rate during hypoxia, reaching a maximum level at the start of hypoxic respiratory depression, suggesting that strong RTN excitation depends on the activation of central hypoxic mechanisms (Bodineau *et al.* 2000*b*). Furthermore, central CO hypoxia, which caused a steady decrease in O_2 delivery to tissues without activating peripheral O_2 chemoreceptors, increases *c-fos* expression in the middle and medial VMS (Bodineau & Larnicol, 2001). As anoxia did not change *c-fos* expression in medial VMS neurons following the reduction of synaptic transmission *in vitro*, the activation of these neurons may require intact synaptic transmission. Neuronal activation in the medial VMS, which is thought to be the PP (Connely *et al.* 1989; Berquin *et al.* 2000; Pelaez *et al.* 2002; Stornetta *et al.* 2005), may be driven by excitation of the hypoxia-sensing neurons of the middle VMS. Indeed, we found that selective destruction of the middle VMS abolished the increase in *c-fos* expression in the medial VMS in anoxic conditions. In this way, tracing studies might provide evidence of medial VMS neuron activation by the contralateral middle VMS neurons (Cream *et al.* 2002). In addition, the perifacial RTN/pFRG VMS is the only region in brainstem–spinal cord preparations that displays an increase in *c-fos* expression in anoxic conditions and is likely to activate medial VMS neurons (Bodineau *et al.* 2001; Voituron *et al.* 2005). An alternative possibility is the presence of hypoxia-sensing neurons that do not express the *c-fos* gene in anoxic conditions, in another brainstem region.

The hypoxia-sensing neurons of the middle VMS are glutamatergic and project onto the pre-Bötzinger complex (Weston *et al.* 2004). Our data suggest that they exert a negative effect on central respiratory drive in anoxia. The excitatory pathway described by Weston *et al.* (2004) is therefore unlikely to be responsible for the observed effect. It is more likely that middle VMS neurons excite the medial VMS neurons responsible for moderating Rf (Fig. 8). This hypothesis is supported by the following observations: (i) similar respiratory responses to anoxia were observed following selective destruction of the middle and medial VMS; (ii) selective destruction of the middle VMS abolished the increase in *c-fos* expression in the medial VMS in anoxic conditions; (iii) projections from the middle VMS to the medial VMS have been observed (Cream *et al.* 2002); (iv) projections from the medial VMS to the rostral ventral respiratory group have been observed (Holtman *et al.* 1990); and (v) the detection of GAD-67 mRNA is consistent with the GABAergic nature

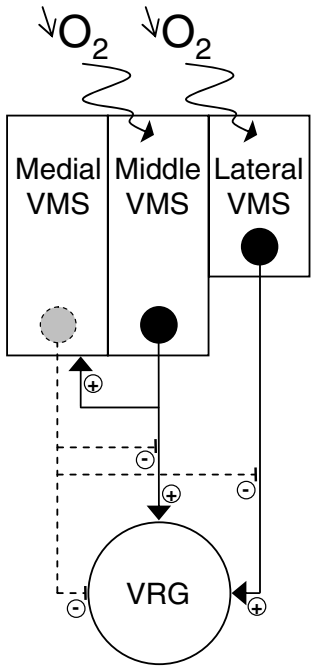

Figure 8. Schematic diagram showing the possible involvement of superficial ventral respiration-related structures in hypoxic respiratory adaptation
The lateral and middle parts of the VMS (perifacial RTN/pFRG area) are thought to have hypoxia-sensing properties, whereas no such properties are ascribed to the medial part of the VMS. In low O_2 conditions, lateral VMS neurons seem to exert a direct positive influence on respiratory drive. By contrast, the middle and medial VMS neurons seem to co-operate in the decrease in respiratory drive observed in anoxic conditions. Hence, the possible direct influence of the middle VMS, as suggested by previous studies (Weston *et al.* 2004), is overcome by the moderating effect of the middle/medial VMS.

of the medial VMS neurons (see Fig. 2*B* in Weston *et al.* 2004; Stornetta *et al.* 2005). Serotoninergic medial VMS neurons have been described (Erickson & Millhorn, 1994; Stornetta *et al.* 2005), and may be involved in hypoxic respiratory adaptation. Nevertheless, this seems unlikely here because, as previously reported, serotoninergic systems are not involved in hypoxic respiratory adaptation in brainstem–spinal cord preparations (Cayetanot *et al.* 2001). As anoxic *c-fos* expression in the middle and lateral VMS is similar in the presence of reduced and active synaptic transmission, medial VMS inhibition is unlikely to have a direct effect on perifacial RTN/pFRG somata neurons (Fig. 8). Medial VMS neurons may directly inhibit ventral respiratory neurons and/or perifacial RTN/pFRG axonal excitatory projections by presynaptic modulation. Finally, the suggested hypoxic coupling between the middle and medial VMS has no effect on the previously reported strong hypercapnic respiratory stimulant effect of the middle VMS (Guyenet *et al.* 2005*a*). This apparent discrepancy may be due to two different middle VMS neuron populations. Further studies on the molecular basis of hypoxia detection should clarify this point.

In conclusion, our study identifies perifacial RTN/pFRG VMS hypoxia-sensing neurons, and a *trans*-synaptic activated area, the medial VMS. Specific lesioning experiments suggest that these areas have different roles, at least in neonates. Middle VMS lesioning revealed anoxic excitation as effectively as medial VMS lesioning. As the increase in *c-fos* expression in the medial VMS seems to depend on the presence of the middle VMS, we suggest that the excitatory middle VMS neurons (Weston *et al.* 2004) are responsible for activating the medial VMS neurons, thereby mediating hypoxic inhibition. In the absence of the middle VMS, the intact hypoxia-sensing neurons of the lateral part of the VMS fully stimulate respiratory drive.

References

Beitz AJ (1995). Periaqueductal gray. In *The Rat Nervous System*, 2nd edn, ed. Paxinos G, pp. 173–182. Academic Press, San Diego.

Belegu R, Hadziefendic S, Dreshaj IA, Haxhiu MA & Martin RJ (1999). CO_2-induced *c-fos* expression in medullary neurons during early development. *Respir Physiol* **117**, 13–28.

Berquin P, Cayetanot F, Gros F & Larnicol N (2000). Postnatal changes in Fos-like immunoreactivity evoked by hypoxia in the rat brainstem and hypothalamus. *Brain Res* **877**, 149–159.

Blessing WW (2005). BAT control shows the way: medullary raphe/parapyramidal neurons and sympathetic regulation of brown adipose tissue. *Am J Physiol Regul Integr Comp Physiol* **288**, 557–560.

Bodineau L, Cayetanot F & Frugière A (2000*a*). Possible role of retrotrapezoid nucleus and parapyramidal area in the respiratory response to anoxia: an *in vitro* study in neonatal rat. *Neurosci Lett* **295**, 67–69.

Bodineau L, Cayetanot F & Frugière A (2001). Fos study of ponto-medullary areas involved in the *in vitro* hypoxic respiratory depression. *Neuroreport* **12**, 3913–3916.

Bodineau L, Frugière A, Marlot D & Wallois F (2000*b*). Effect of hypoxia on the activity of respiratory and non respiratory modulated retrotrapezoid neurons of the cat. *Auton Neurosci* **86**, 70–77.

Bodineau L & Larnicol N (2001). Brainstem and hypothalamic areas activated by tissues hypoxia: Fos-like immunoreactivity induced by carbon monoxide inhalation in the rat. *Neuroscience* **108**, 643–653.

Borday C, Wrobel L, Fortin G, Champagnat J, Thaeron-Antono C & Thoby-Brisson M (2004). Developmental gene control of brainstem function: views from the embryo. *Prog Biophys Mol Biol* **84**, 89–106.

Brockhaus J, Ballanyi K, Smith JC & Richter DW (1993). Microenvironment of respiratory neurons in the *in vitro* brainstem–spinal cord of neonatal rats. *J Physiol* **462**, 421–445.

Cayetanot F, Bodineau L & Frugière A (2001). 5-HT acting on 5-$HT_{1/2}$ receptors does not participate in the *in vitro* hypoxic respiratory depression. *Neurosci Res* **41**, 71–78.

Connelly CA, Ellenberger HH & Feldman JL (1989). Are there serotoninergic projections from raphe and retrotrapezoid nuclei to the ventral respiratory group in the rat? *Neurosci Lett* **105**, 34–40.

Cream C, Li A & Nattie EE (2002). The retrotrapezoid nucleus (RTN): local cytoarchitecture and afferent connections. *Respir Physiol Neurobiol* **130**, 121–137.

Dillon GH, Welsh DE & Waldrop TG (1991). Modulation of respiratory reflexes by an excitatory amino acid mechanism in the ventrolateral medulla. *Respir Physiol* **85**, 55–72.

Dragunow M & Faull R (1989). The use of *c-fos* as a metabolic marker in neuronal pathway tracing. *J Neurosci Meth* **29**, 261–265.

Ellenberger HH & Feldman JL (1990). Brainstem connections of the rostral ventral respiratory group of the rat. *Brain Res* **513**, 35–42.

Erickson JT & Millhorn DE (1994). Hypoxia and electrical stimulation of the carotid sinus nerve induce Fos-like immunoreactivity within catecholaminergic and serotoninergic neurons of the rat brainstem. *J Comp Neurol* **348**, 161–182.

Gourine AV, Llaudet E, Dale N & Spyer KM (2005). Release of ATP in the ventral medulla during hypoxia in rats: role in hypoxic ventilatory response. *J Neurosci* **25**, 1211–1218.

Guyenet PG, Mulkey DK, Stornetta RL & Bayliss DA (2005*a*). Regulation of ventral surface chemoreceptors by the central respiratory pattern generator. *J Neurosci* **25**, 8938–8947.

Guyenet PG, Stornetta RL, Bayliss DA & Mulkey DK (2005*b*). Retrotrapezoid nucleus: a litmus test for the identification of central chemoreceptors. *Exp Physiol* **90**, 247–253.

Hausmann A, Marksteiner J, Hinterhuber H & Humpel C (2001). Magnetic stimulation induces neuronal *c-fos* via tetrodotoxin-sensitive sodium channels in organotypic cortex brain slices of the rat. *Neurosci Lett* **310**, 105–108.

Herdegen T, Kovary K, Leah J & Bravo R (1991). Specific temporal and spatial distribution of JUN, FOS, and KROX-24 proteins in spinal neurons following noxious transsynaptic stimulation. *J Comp Neurol* **313**, 178–191.

Herdegen T & Leah JD (1998). Inducible and constitutive transcription factors in the mammalian nervous system: control of gene expression by Jun, Fos and Krox, and CREB/ATF proteins. *Brain Res Brain Res Rev* **28**, 370–490.

Hilaire G, Monteau R & Errchidi S (1989). Possible modulation of the medullary respiratory rhythm generator by the noradrenergic A5 area: an *in vitro* study in the newborn rat. *Brain Res* **485**, 325–332.

Hilaire G, Viemari JC, Coulon P, Simonneau M & Bévengut M (2004). Modulation of the respiratory rhythm generator by the pontine noradrenergic A5 and A6 groups in rodents. *Respir Physiol Neurobiol* **143**, 187–197.

Holtman JR, Marion LJ & Speck DF (1990). Origin of serotonin-containing projections to the ventral respiratory group in the rat. *Neuroscience* **37**, 541–552.

Janczewski WA & Feldman JL (2006). Distinct rhythm generators for inspiration and expiration in the juvenile rat. *J Physiol* **570**, 407–420.

Kawai A, Onimaru H & Homma I (2006). Mechanisms of CO_2/H^+ chemoreception by respiratory rhythm generator neurons in the medulla from newborn rats *in vitro*. *J Physiol* **572**, 525–537.

Lanteri-Minet M, Weil-Fugazza J, de Pommery J & Menetrey D (1994). Hindbrain structures involved in pain processing as revealed by the expression of *c-fos* and other immediate early gene proteins. *Neuroscience* **58**, 287–298.

Larnicol N, Wallois F, Berquin P, Gros F & Rose D (1994). *c-fos* like immunoreactivity in the cat's neuraxis following moderate hypoxia or hypercapnia. *J Physiol Paris* **88**, 81–88.

Li A & Nattie EE (2002). CO_2 dialysis in one chemoreceptor site, the RTN: stimulus intensity and sensitivity in the awake rat. *Respir Physiol Neurobiol* **133**, 11–22.

López-Barneo J, Del Toro R, Levitsky KL, Chiara MD & Ortega-Sáenz P (2004). Regulation of oxygen sensing by ion channels. *J Appl Physiol* **96**, 1187–1195.

Marina N, Morales T, Díaz N & Mena F (2002). Suckling-induced activation of neural *c-fos* expression at lower thoracic rat spinal cord segments. *Brain Res* **954**, 100–114.

Mellen NM, Janczewski WA, Bocchiaro CM & Feldman JL (2003). Opioid-induced quantal slowing reveals dual network for respiratory rhythm generation. *Neuron* **37**, 821–826.

Mironov SL, Hartelt N & Ivannikov MV (2005). Mitochondrial K_{ATP} channels in respiratory neurons and their role in the hypoxic facilitation of rhythmic activity. *Brain Res* **1033**, 20–27.

Mitchell RA, Loeschcke HH, Massion WH & Severinghaus JW (1963). Respiratory responses mediated through superficial chemosensitive areas on the medulla. *J Appl Physiol* **18**, 523–533.

Morgan JI, Cohen DR, Hempstead JL & Curran T (1987). Mapping patterns of *c-fos* expression in the central nervous system after seizure. *Science* **237**, 192–197.

Mulkey DK, Stornetta RL, Weston MC, Simmons JR, Parker A, Bayliss DA & Guyenet PG (2004). Respiratory control by ventral surface chemoreceptor neurons in rats. *Nat Neurosci* **7**, 1360–1369.

Nattie E (1999). CO_2, brainstem chemoreceptors and breathing. *Progr Neurobiol* **59**, 299–331.

Neubauer JA & Sunderram J (2004). Oxygen-sensing neurons in the central nervous system. *J Appl Physiol* **96**, 367–374.

Okada Y, Chen Z, Jiang W, Kuwana S & Eldridge FL (2002). Anatomical arrangement of hypercapnia-activated cells in the superficial ventral medulla of rats. *J Appl Physiol* **93**, 427–439.

Okada Y, Kawai A, Mückenhoff K & Scheid P (1998). Role of the pons in the hypoxic respiratory depression in the neonatal rat. *Respir Physiol* **111**, 55–63.

Okada Y, Mückenhoff K, Holtermann G, Acker H & Scheid P (1993). Depth profiles and PO_2 in the isolated brain stem-spinal cord of the neonatal rat. *Respir Physiol* **93**, 315–326.

Onimaru H, Arata A, Arata S, Shirasawa S & Cleary ML (2004). *In vitro* visualization of respiratory neuron activity in the newborn mouse ventral medulla. *Brain Res Dev Brain Res* **153**, 275–279.

Onimaru H & Homma I (2003). A novel functional neuron group for respiratory rhythm generation in the ventral medulla. *J Neurosci* **23**, 1478–1486.

Onimaru H, Kumagawa Y & Homma I (2006). Respiration-related rhythmic activity in the rostral medulla of newborn rats. *J Neurophysiol* **96**, 55–61.

Overholt JL, Ficker E, Yang T, Shams H, Bright GR & Prabhakar NR (2000). HERG-like potassium current regulates the resting membrane potential in glomus cells of the rabbit carotid body. *J Neurophysiol* **83**, 1150–1157.

Patel AJ & Honore E (2001). Molecular physiology of oxygen-sensitive potassium channels. *Eur Respir J* **18**, 221–227.

Pearce RA, Stornetta RL & Guyenet PG (1989). Retrotrapezoid nucleus in the rat. *Neurosci Lett* **101**, 138–142.

Pelaez NM, Schreihofer AM & Guyenet PG (2002). Decompensated hemorrhage activates serotoninergic neurons in the subependymal parapyramidal region of the rat medulla. *Am J Physiol Regul Integr Comp Physiol* **283**, 688–697.

Pena F, Parkis MA, Tryba AK & Ramirez JM (2004). Differential contribution of pacemaker properties to the generation of respiratory rhythms during normoxia and hypoxia. *Neuron* **43**, 105–117.

Reis DJ, Golanov EV, Ruggiero DA & Sun MK (1994). Sympatho-excitatory neurons of the rostral ventrolateral medulla are oxygen sensors and essential elements in the tonic and reflex control of the systemic and cerebral circulations. *J Hypertens Suppl.* **12**, 159–180.

Saadani-Makki F, Frugière A, Gros F, Gaytán S & Bodineau L (2004). Involvement of adenosinergic A_1 systems in the occurrence of respiratory perturbations encountered in newborns following an *in utero* caffeine exposure: a study on brainstem-spinal cord preparations isolated from newborn rats. *Neuroscience* **127**, 505–518.

Sagar SM, Sharp FR & Curran T (1988). Expression of *c-fos* protein in brain: metabolic mapping at the cellular level. *Science* **240**, 1328–1331.

Simerly RB (1995). Anatomical substrate of hypothalamic integration. In *The Rat Nervous System*, 2nd edn, ed.Paxinos G, pp. 353–376. Academic Press, San Diego.

Smith JC, Morrison DE, Ellenberger HH, Otto MR & Feldman JL (1989). Brainstem projections to the major respiratory population in the medulla of the cat. *J Comp Neurol* **281**, 69–96.

Solomon IC, Edelman NH & Neubauer JA (2000). Pre-Botzinger complex functions as a central hypoxia chemosensor for respiration *in vivo*. *J Neurophysiol* **83**, 2854–2868.

Stornetta RL, Rosin DL, Simmons JR, McQuiston TJ, Vujovic N, Weston MC & Guyenet PG (2005). Coexpression of vesicular glutamate transporter-3 and aminobutyric acidergic markers in rat rostral medullary raphe and intermediolateral cell column. *J Comp Neurol* **492**, 477–494.

Sun MK & Reis DJ (1994). Hypoxia-activated Ca^{2+} currents in pacemaker neurones of rat rostral ventrolateral medulla *in vitro*. *J Physiol* **476**, 101–116.

Suzue T (1984). Respiratory rhythm generation in the *in vitro* brainstem-spinal cord preparation of the neonatal rat. *J Physiol* **354**, 173–183.

Takakura ACT, Moreira TS, Colombari E, West GH, Stornetta RL & Guyenet PG (2006). Peripheral chemoreceptor inputs to retrotrapezoid nucleus (RTN) CO_2-sensitive neurons in rats. *J Physiol* **572**, 503–523.

Teppema LJ, Veening JG, Kranenburg A, Dahan A, Berkenbosch A & Olievier C (1997). Expression of *c-fos* in the rat brainstem after exposure to hypoxia and to normoxic and hyperoxic hypercapnia. *J Comp Neurol* **388**, 169–190.

Vizek M, Pickett CK & Weil JV (1987). Biphasic ventilatory response of adult cats to sustained hypoxia has central origin. *J Appl Physiol* **63**, 1658–1664.

Voituron N, Frugière A, Gros F, Macron JM & Bodineau L (2005). Diencephalic and mesencephalic influences on ponto-medullary respiratory control in normoxic and hypoxic conditions. An *in vitro* study on central nervous system preparations from newborn rat. *Neuroscience* **132**, 843–854.

Weston MC, Stornetta RL & Guyenet PG (2004). Glutamatergic neuronal projections from the marginal layer of the rostral ventral medulla to the respiratory centers in rats. *J Comp Neurol* **473**, 73–85.

Acknowledgements

We thank Drs A. Gallet and J. Rochette for valuable comments on the manuscript and Alex Edelman and associates for correcting the English.